

Effect of Poling Direction on *R*-Curve Behavior in Lead Zirconate Titanate

Sergio L. dos Santos e Lucato, Doru C. Lupascu,* and Jürgen Rödel*

Department of Materials Science, Darmstadt University of Technology, D-64287 Darmstadt, Germany

***R*-curves of lead zirconate titanate (PZT) have been measured with compact tension (CT) specimens for different poling conditions and grain sizes. Depending on poling direction the plateau value of the *R*-curves ranged from 1.13 to 1.54 MPa·m^{1/2} for a grain size of 6.4 μm and from 1.14 to 1.30 MPa·m^{1/2} for a grain size of 5.2 μm. Poling in the thickness direction yielded the material with the highest fracture toughness while the direction parallel to the loading direction led to the lowest fracture toughness.**

I. Introduction

THE increasing use of piezoceramic actuators requires a good knowledge of the fracture behavior of the materials employed. As the PZT system shows a particularly large electromechanical strain near the morphotropic phase boundary, it is of special interest for actuator applications.

From past investigations using short cracks, which were produced with Vickers or Knoop indentations, it is well known that electrically poled piezoelectric ceramics exhibit a strongly anisotropic fracture toughness.^{1,2} This is mainly attributed to the different switching ability of domains lying in the crack tip stress field. Both poling direction as well as degree of polarization have to be considered. While most investigations focused on indentation techniques, only very few publications on *R*-curve behavior in ferroelectric materials are known.^{3–5} The question of the full influence of poling, however, has not been addressed yet. Previous researchers agreed that toughening is attributed to a process zone mechanism similar to transformation toughening,^{3,6} with domain orientation being an additional complicating feature in ferroelastic switching.

In this work the influence of the polarization orientation was investigated for two grain sizes. A systematic analysis for long cracks was possible using compact tension specimens that were poled along the respective edges and compared to the unpoled material.

II. Experimental Procedure

(1) Sample Preparation and Poling

All experiments were performed on a commercially available lead zirconate titanate, namely PZT 151 (PI Ceramics, Lederhose, Germany). The samples were delivered as plates of dimensions

50 × 48 × 3 mm³ and were polished on one side to a 1 μm finish. The distribution of grain sizes has been reported before.⁷

To ensure identical chemical compositions of the two batches of different grain sizes, an X-ray fluorescence analysis (XFA) was performed determining the relative concentrations.

The electrodes for poling were silver painted onto the sample surfaces. The specimens were then poled with a field of 1.8E_c (with E_c = 1 kV/mm this required up to 90 kV for the largest dimension). Particular care had to be taken to avoid breakdown at these high voltages. A special poling device was built using components of Fischertechnik® (Construction-set of Nylon®) and kept in a plastic bucket filled with silicone oil. A coordinate system describing the poling direction was used as follows. Direction *A* is the crack growth direction. *B* and *C* are parallel to the thickness direction and the loading axis, respectively. Unpoled specimens are termed *X*.

(2) Electrical and Optical Analysis

After poling the electrodes were carefully removed with acetone and two holes were drilled for specimen fixture.

The material from the bore holes had a diameter of approximately 7 mm and was used to determine the strain and dielectrical displacement hysteresis. The strain was measured with a linear inductive displacement transducer (LVDT). A field of up to 2 kV/mm was applied for the hysteresis measurement.

Some of the removed material was chemically etched on the polished surface. The acid consisted of a mixture of HF and HCl. The grain sizes were measured conforming to the linear intercept technique described in Ref. 8 with a custom-designed software program⁹ on optical micrographs of magnification 1000×.

(3) *R*-Curve Measurement

The CT-testing device was a new version of the type used before¹⁰ and was mounted on a coordinate stage on an optical microscope.

Prior to the *R*-curve measurement a sharp precrack was produced using a half chevron notch and a Knoop indent with load of 50 N as described in Ref. 10. After the precrack had been driven through the region of the half chevron notch, it was then renotched to a final length of approximately 50–150 μm. The test itself was performed according to ASTM 399.¹¹ As the size of the plastic zone in PZT is much smaller than the sample thickness, the equation for calculating the stress intensity factor according to ASTM 399 was also applied. Data sets consisted of applied load and crack length at the onset of crack propagation. To ensure maximum reproducibility, special care was taken to record data at crack velocities at about 10⁻⁵ m/s. After every data point the load was reduced until the crack stopped. In order to reduce the effects of material relaxation about 30 s of holding time was allowed before reloading.

D. Munz—contributing editor

Manuscript No. 189121. Received September 2, 1999; approved November 15, 1999.

Supported by the Deutsche Forschungsgemeinschaft (DFG) under Contract No. Rö 954/13-1.

*Member, American Ceramic Society.

III. Results and Discussion

(1) Microstructure and Electrical Characteristics

Within the measuring accuracy of the XFA the raw materials proved identical. The differences in the structures are attributed to a slightly different sintering process. The mean grain sizes for both batches were 6.4 and 5.2 μm , respectively.

A clear difference exists between the samples of both grain sizes concerning maximum and remanent strain. The strain hysteresis for both grain sizes is provided in Fig. 2 and shown to differ by approximately 20%. For better comparability the curves are plotted relative to their minimum values. The maximum strain for the larger grains is around 0.4% and 0.33% for the smaller grains. Comparable results are obtained for the remanent strain (0.25% versus 0.18%). The observed effect of grain size is in good agreement with previous publications.¹² The coercive field of 1 kV/mm is identical for both grain sizes.

(2) R-Curve Behavior

The cracking behavior significantly depended on the different poling directions of the material. Only a few small bridges could be seen in the crack path with bridging widths of around 1–2 grains for the B-poled specimens. More and bigger crack bridges were observed in the unpoled and the A-poled samples. Here, bridges were observed with widths of up to 100 μm . Many bridges with magnitudes of up to 500 μm were observed in the C direction.

The behavior of the A specimens is of special interest. Switching in that configuration leads to a strain incompatibility between the process zone and the bulk of the specimen. Therefore, an increase in the stress in the direction of the crack propagation and a decrease in the stress perpendicular to it are obtained. The stresses in crack propagation direction yielded many cracks oriented perpendicular to the main crack. These cracks were located at the end of the specimen with respect to the direction of the crack growth and had a length of several millimeters as indicated in Fig. 1.

Figure 1 compares specimens exhibiting the four poling states. The starting values for the R-curves could not be given with good accuracy, as tempering after crack initiation would have depoled the sample. A steep rise at the beginning of the R-curve is observed for all poling directions with the final value being almost reached after about 0.5 to 1 mm. From this crack length to a crack length of about 3 mm, materials of all poling directions showed a further increase in toughness of about 0.1 to 0.2 $\text{MPa}\cdot\text{m}^{1/2}$. In this crack length regime, the material poled in the C direction exhibited the most toughening, if all specimens investigated are taken into account. This is consistent with optical observations of bridge densities and the size of the bridges. These final toughness values are termed plateau values and are provided in Table I. Specimens,

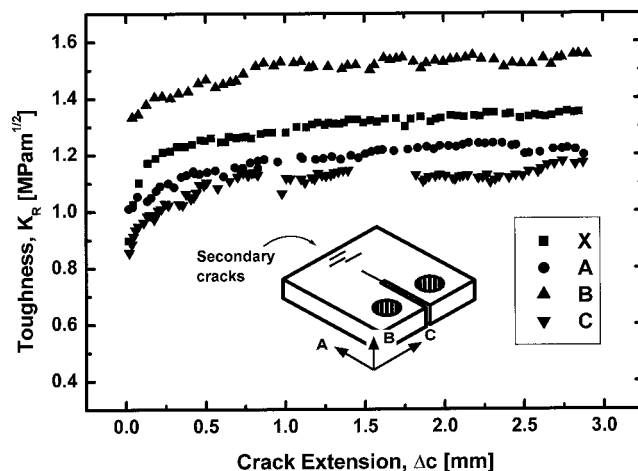


Fig. 1. R-curves for specimens with three different poling directions as contrasted to an unpoled specimen. The secondary cracks formed for the A-type specimens are indicated.

Table I. Plateau Values for Fracture Toughness for Two Grain Sizes and Four Poling States

Poling state	K_{IC} ($\text{MPa}\cdot\text{m}^{1/2}$)	
	Large grains	Small grains
X (unpoled)	1.30	1.13
A	1.22	
B	1.54	1.28
C	1.13	1.14

which were unloaded to 10% of the load at crack equilibrium and were held for 15 min, exhibited toughness values between 0.8 and 1.0 $\text{MPa}\cdot\text{m}^{1/2}$ upon repropagation. As ferroelastic toughening was demonstrated to be time dependent,³ it is therefore suggested that ferroelastic toughening is the major toughening effect. In contrast, crack bridging constitutes only the minor part of the toughening and in particular the toughness increases for cracks larger than 0.5 to 1.0 mm.

R-curves on the identical material in one poling direction as well as for unpoled material have been obtained in edge notched bending bars by Fett *et al.*⁴ In their work, fracture toughness values between 1.2 and 1.5 $\text{MPa}\cdot\text{m}^{1/2}$, comparable to our work, have been reported. As the crack lengths were only 500 μm , no plateau values could be obtained. The advantage of the CT specimen is the large notch length, which allows considerable crack extension with large attendant long-range R-curve behavior. Therefore, large-scale bridging or large process zones, which would prohibit attainment of a measurable steady-state toughness, are not encountered.¹³

The highest plateau of 1.5 $\text{MPa}\cdot\text{m}^{1/2}$ starting from 0.8 $\text{MPa}\cdot\text{m}^{1/2}$ can be found for the B-poling. Domain switching is easily possible in this configuration. The R-curve for C-poling starts at 0.8 $\text{MPa}\cdot\text{m}^{1/2}$ and extends to a final value of 1.1 $\text{MPa}\cdot\text{m}^{1/2}$, providing clearly the least toughening. As most domains are orientated in the loading direction due to poling, very little reinforcement can be contributed from domain switching. Some reinforcement is still possible as not all domains are aligned by poling. To reduce misfit stresses between adjacent grains some domains switch back after removing the poling field at the end of the poling process. The crack tip stress field of the approaching crack now also switches these domains. The fracture toughness of the unpoled samples, which ranges from 0.9 to 1.3 $\text{MPa}\cdot\text{m}^{1/2}$, is between B and C. The A-state achieves a final fracture toughness of 1.2 $\text{MPa}\cdot\text{m}^{1/2}$. The difference in the C-state is only marginal. Theoretically the domains should be able to switch as they are not oriented parallel to the principal stress direction. However, because of mechanical clamping by the full sample length in the A direction, switching is limited. Our results with respect to the toughness ranking between directions A and B cannot be generalized. Toughening with poled samples in either of these two directions is expected to sensitively depend on specimen thickness and uncracked ligament length normalized by the process zone. Also the stress state plays a crucial role in determining the extent of ferroelastic toughening.⁵ Chen *et al.*⁵ suggested that the main toughening mechanism is the domain switching. SCF measurements (surface crack in flexure¹⁴) on PLZT provided only R-curve behavior in the ferroelastic composition while the linear-elastic PLZT exhibited a constant fracture toughness.

The effect of grain size was compared for the B- and C-poled specimens as well as for unpoled samples. The result for the B-state is shown in Fig. 2. Larger grains exhibit a significantly higher fracture toughness for the same poling conditions. The effect is best seen in the B-poled samples because that direction has the most efficient domain switching. As the C-poled specimens exhibit only limited domain switching, no influence of the grain size could be measured. A summary of the fracture toughness values for PZT 151 for different poling states and grain sizes is finally provided in Table I. A quantitative understanding of the poling effects is beyond the scope of this work and would require

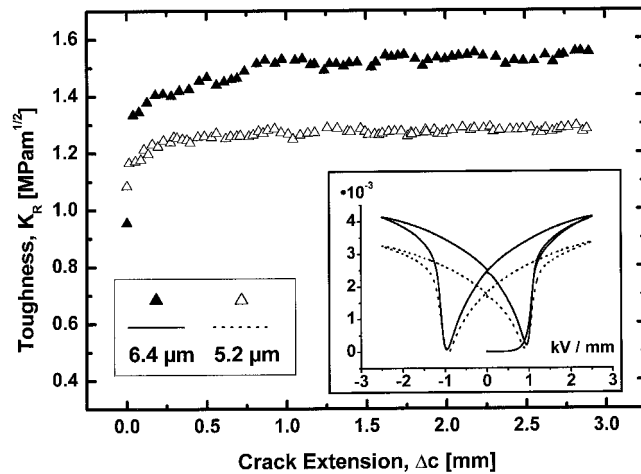


Fig. 2. R -curves for two different grain sizes with poling direction B along with the strain hysteresis for grain sizes of 5.2 and 6.4 μm .

not only inclusion of effects of poling, but also consideration of specimen dimensions as compared to the size of the process zone.

IV. Conclusions

- (1) Poling direction has a significant influence on the plateau value of the R -curve as obtained in CT specimens. The toughening efficiency ranked in the following order of poling direction: $B > X > A > C$.
- (2) Mechanical clamping due to specimen geometry leads to the formation of secondary cracks far away from and perpendicular to the main crack.
- (3) An increase in grain size yields an increase in remanent strain and an increase in toughening.

Acknowledgments

We would like to thank Nils Hardt from the Institut für Hochspannungstechnik for his help with the high-voltage source.

References

- ¹K. Okazaki, "Mechanical Behavior of Ferroelectric Ceramics," *Am. Ceram. Soc. Bull.*, **63** [9] 1150–52 (1984).
- ²G. G. Pisarenko, V. M. Chushko, and S. P. Kovalev, "Anisotropy of Fracture Toughness of Piezoelectric Ceramics," *J. Am. Ceram. Soc.*, **68** [5] 259–65 (1985).
- ³F. Meschke, A. Kolleck, and G. A. Schneider, " R -Curve Behaviour of BaTiO_3 Due to Stress-Induced Ferroelastic Domain Switching," *J. Eur. Ceram. Soc.*, **17**, 1143–49 (1997).
- ⁴T. Fett, D. Munz, and G. Thun, "Fracture Toughness and R -Curve Behaviour of PZT," *Wiss. Ber. Forschungszentrums Karlsruhe*, 6058 (1998).
- ⁵W. Chen, D. C. Lupascu, J. Rödel, and C. S. Lynch, "A Comparison of the Short Crack in Flexure R -Curve Behavior of Unpoled Ferroelectric 8/65/35 and Quadratic Electrostrictor 9.5/65/35 PLZT," unpublished work.
- ⁶K. Mehta and A. V. Virkar, "Fracture Mechanisms in Ferroelectric–Ferroelastic Lead Zirconate Titanate ($\text{Zr}:\text{Ti} = 0.54:0.46$) Ceramics," *J. Am. Ceram. Soc.*, **73** [3] 567–74 (1990).
- ⁷J. Nuffer, D. C. Lupascu, and J. Rödel, "Acoustic Emission in PZT under Bipolar Electric Driving and Uniaxial Mechanical Stress," *Ferroelectrics*, in press.
- ⁸"Standard Test Method for Determining Average Grain Size," E112–96; pp. 227–49 in *Annual Book of ASTM Standards*, 3.01. American Society for Testing and Materials, West Conshohocken, PA, 1997.
- ⁹S. L. dos Santos e Lucato, "Lince v2.4—Linear Intercept," Department of Materials Science, Darmstadt University of Technology, Darmstadt, Germany, 1999.
- ¹⁰J. Rödel, J. F. Kelly, and B. R. Lawn, "*In-Situ* Measurement of Bridged Crack Interfaces in the Scanning Electron Microscope," *J. Am. Ceram. Soc.*, **73** [11] 3313–18 (1990).
- ¹¹"Standard Test Method for Plane-Strain Fracture Toughness of Metallic Materials," E399–90; pp. 408–38 in *Annual Book of ASTM Standards*, 3.01. American Society for Testing and Materials, West Conshohocken, PA, 1997.
- ¹²C. A. Randall, N. Kim, J.-P. Kucera, W. Cao, and T. R. Shrout, "Intrinsic and Extrinsic Size Effects in Fine-Grained Morphotropic-Phase-Boundary Lead Zirconate Titanate Ceramics," *J. Am. Ceram. Soc.*, **81** [3] 677–88 (1998).
- ¹³B. D. Flinn, C. S. Lo, F. W. Zok, and A. G. Evans, "Fracture Resistance Characteristic of a Metal-Toughened Ceramic," *J. Am. Ceram. Soc.*, **76** [2] 369–75 (1993).
- ¹⁴M. Stech and J. Rödel, "Method for Measuring Short-Crack R -Curves without Calibration Parameters: Case Studies on Alumina and Alumina/Aluminium Composites," *J. Am. Ceram. Soc.*, **79** [2] 291–97 (1996). □